Journal of Applied Engineering Mathematics

Volume 2

1D MOMENTUM INTEGERAL METHOD (THWAITES) VS. 2D FINITE ELEMENT NAVIER-STOKES SOLUTION: COMPUTING FLOW SEPERATION, FLOW RATE AND PRESSURE DROP

Gifford Zach Decker

Mechanical Engineering Department
Brigham Young University
Provo,Utah 84602

ABSTRACT

The human vocal folds have been modeled many different ways. However, the aerodynamic forces are consistently modeled using 1 of 2 approaches: 1. The Navier-Stokes (NS) equation 2. A simplified Bernoulli equation. Computational fluid dynamics (CFD) using finite element analysis (FEA) implement the NS equations. In this research a user supplied subroutine (USL) was provided in the CFD program ADINA (Automatic Dynamic Incremental Nonlinear Analysis) that implements a 1D momentum integral (MI) approach to finding the point of flow separation and numerically integrates and differentiates the governing equations to provide the aerodynamic forces along the surface of the vocal fold. Four different static cases were run. For each case three parameters were compared between the 2D FEA and the 1D MI approach:

1. Predicted point of flow separation.
2. Predicted Volumetric Flow Rate.
3. Predicted Pressure Drop.

The results provide a conclusion that the USL can be used in place of the FEA while maintaining sufficient accuracy.

NOMENCLATURE

Q Volumetric Flow Rate
fs Point of flow separation

INTRODUCTION

The purpose of this research is to determine if a more simple approach to determining aerodynamic forces can provide an accurate model comparable to that provided by a 2D FEA, so that the simpler model can be implemented in a purely solid domain eliminating the need to discretize the fluid domain. By so doing adhesion between the vocal folds can be modeled without the problem of a collapsing fluid mesh between the folds. This paper outlines a 1D MI approach implemented in the solid domain the results are then compared to the FEA results to determine how accurately the model predicts the flow phenomenon.

The basic geometry of the vocal folds is presented in Fig. 1, the figure represents only half of the channel, with the line of symmetry represented as a dashed line.

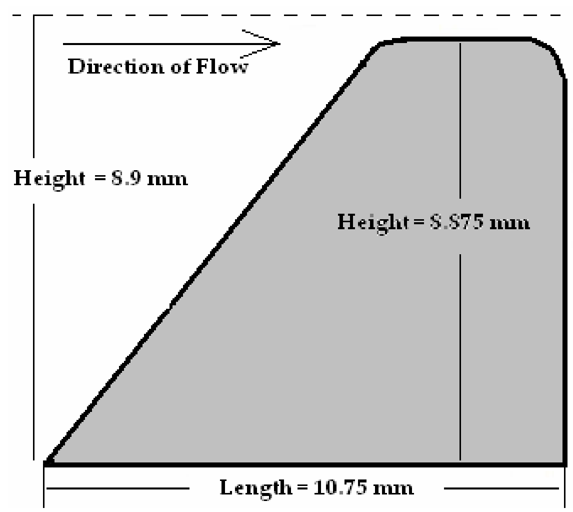

Figure 1: Geometry of the Vocal Fold

For the USL the surface of the fold is discretized and the x and y coordinates of each discretization at each time step is known.

ANALYSIS

Description of the 4 cases

Four different geometries were considered in this study: two straight channels with different heights, height 1 = 0.0178 (fig 2. a), height 2 = 0.169 (fig 2. b), 1 convergent channel (fig(2. c), and 1 divergent channel (fig. 2. d). These four different geometries provide a wide range of pressure drops, fs, and Q.

FEA

The FEA analysis was done by creating a fluid structure interaction with a fluid channel that contained the different geometries[1]. To get a steady, static result the time steps were started very small and increased as the steps increased. This resulted in steady, static flow results for the four different cases.

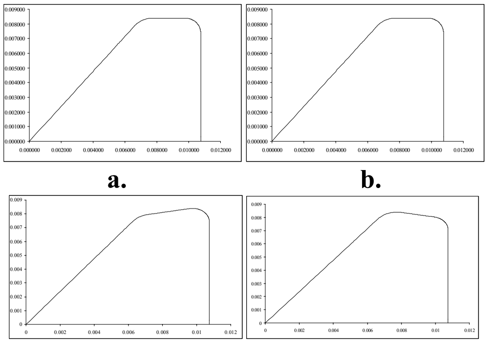

a. b.

c. d.

Figure 2: Different geometries of the folds.

Momentum integral approach

The MI approach that was used is called the correlation method of Thwaites[2]. Thwaites rewrote the Karman equation using the variable lambda (λ), with the following result:

$$\lambda = \frac{\theta^2}{\nu} U' \qquad U' = \frac{dU}{dx} \qquad \text{eq. 1}$$

Thwaites also noted that the momentum thickness θ^2 can be approximated by the following equation[2]:

$$\theta^2 = \frac{0.45\nu}{U^6} \int_0^x U^5 dx \qquad \text{eq. 2}$$

To calculate these values numerical integration and differentiation were used (see Appendix). Once θ^2 was calculated, λ was evaluated and at the point where $\lambda =$ -0.09 the flow was said to have separated.

To converge to the correct Q the fs point was stored and the ratio of the pressure at the fs and the minimum pressure equation 3 was calculated and made to be within -0.05 and 0.05 by changing the Q.

$$\frac{P_{fs}}{P_{min}} \approx 0 \pm 0.05 \qquad \text{eq. 3}$$

RESULTS

Straight Channel H = 17.8 mm

The first case was the straight channel with a nominal height of 17.8 mm (see Fig. 2 a). The comparison of fs is presented in figure 3. The comparison of Q is shown in table 1. The pressure drop comparison is shown in figure 4.

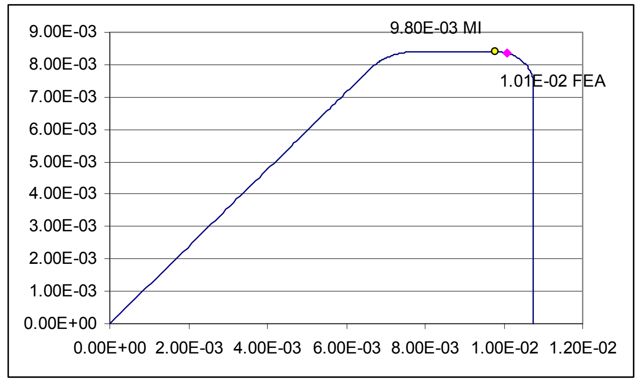

Figure 3: Separation point comparison case 1.

The separation points are within 3% error, the Thwaites method is only guaranteed to provide accuracy of ± 15% close to the separation point. So an accuracy of 3% is very good.

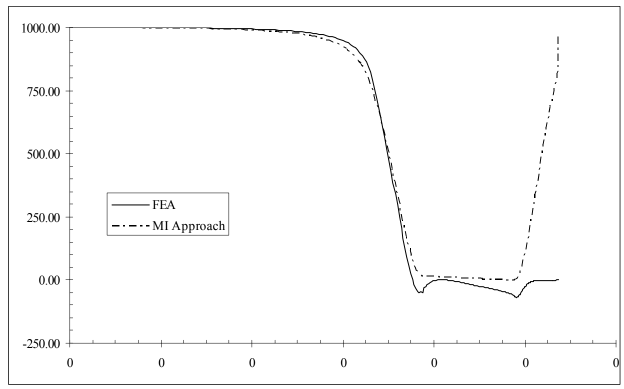

Figure 4: Pressure drop comparison case 1.

The pressure drops are close in behavior, the MI approach recovers the drop completely, because the pressure calculation does not account for the pressure behavior after separation.

Straight Channel H = 16.9 mm

The second case was the straight channel with a narrow gap, nominal height of 16.9 mm (see fig 2 b). The comparison of fs is presented in figure 5. The comparison of Q is shown in table 1. The pressure drop comparison is shown in figure 6.

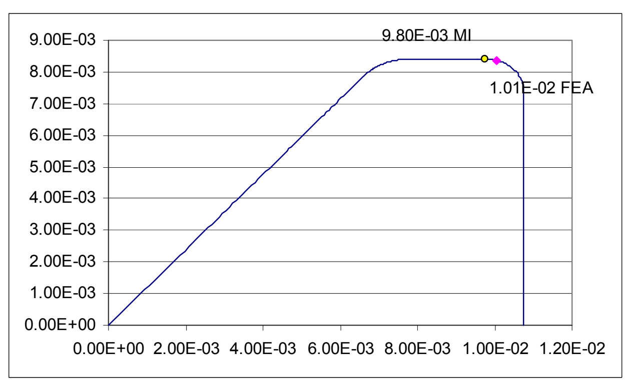

Figure 5: Separation point comparison case 2.

Again the separation point error is within 3% for case 2.

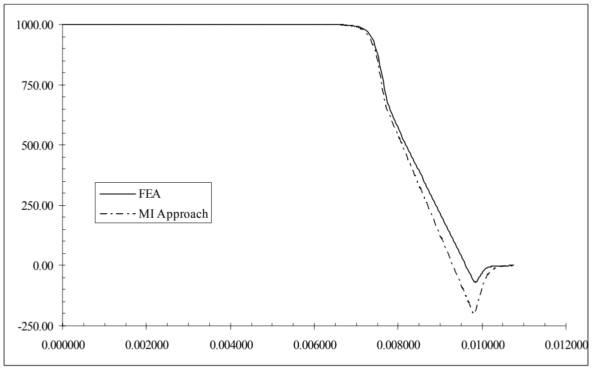

Figure 6: Pressure drop comparison case 2.

The pressure drops for case 2 are also similar in behavior, and the MI approach converges similar to the FEA.

Convergent Channel

The third case was the convergent channel with the height = 17.8 mm (see fig 2 c). The comparison of fs is presented in figure 7. The comparison of Q is shown in table 1. The pressure drop comparison is shown in figure 8.

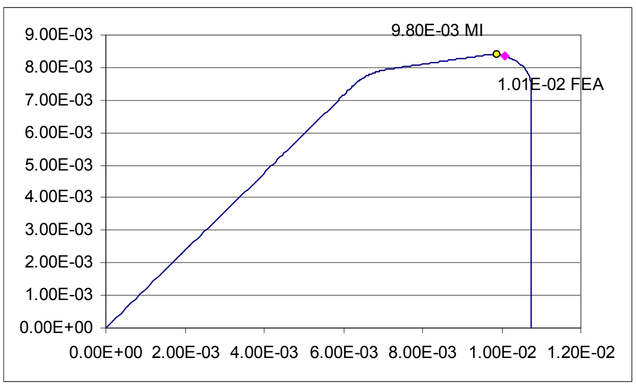

Figure 7: Separation point comparison case 3.

For the convergent channel case 3, the fs error is within 2%, even more accurate than the previous two straight channels.

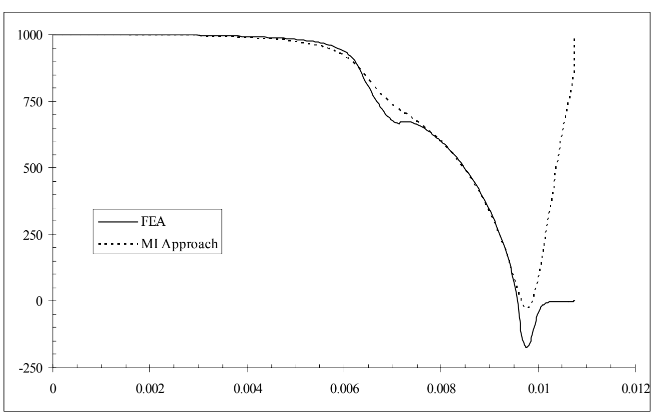

Figure 8: Pressure drop comparison for case 3.

The pressure drop behaviors for the convergent channel are similar; the MI approach does under predict the minimum pressure.

Divergent Channel

The last case was the divergent channel with height = 17.8 mm (see fig 2 d). The comparison of fs is presented in figure 9. The comparison of Q is shown in table 1. The pressure drop comparison is shown in figure 10.

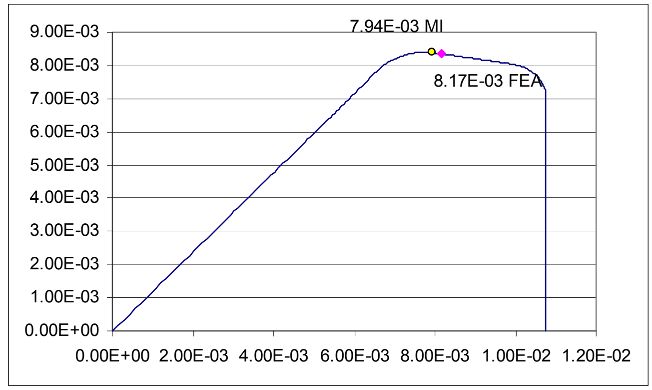

Figure 9: Separation point comparison for case 4.

For the divergent case the fs error is also within 3%.

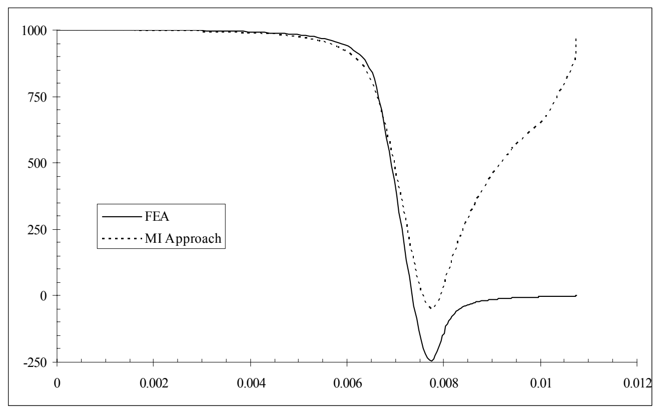

Figure 10: Pressure drop comparison for case 4.

The pressure drop behavior is similar, again the MI under predicts the minimum value of the pressure drop.

Table 1: Flow rate comparison for all cases.

Case #	Flow Rate		Percent error
	FEA	MI	
1	0.037347	0.038570	3.27%
2	0.001619	0.001640	1.28%
3	0.039301	0.039410	0.28%
4	0.040316	0.039850	-1.16%

The flow rates are all within 5% error with the highest error in case 1 at 3.27% and the lowest in case 3 at 0.28%.

CONCLUSIONS

In conclusion, the results for the fs, Q, and the pressure drop for all four cases are very good, and within a range of error percentage that is acceptable. As can be seen from the figures and table the MI maintains a similar behavior for all 4 cases, however, the MI consistently under predicts on the fs. For the Q and pressure drop it is not consistent, for the first three cases the MI over predicts the Q and under predicts on the last case. For the pressure drop, the MI under predicts on cases 1,3, and 4 and over predicts on case 2. With these results and future work on the modeling equations, the aerodynamic forces on the surface of the vocal fold will be successfully modeled in the solid domain. This will allow for the modeling of adhesion and a first look at the stresses and effects that adhesion has on the vocal folds.

ACKNOWLEDGMENTS

I thank first of all my Family, my wife Marci for allowing me to pursue this research and take time from our lives together to ensure that it is done properly. My son, Zachariah who misses his dad and puts of with him when he is at home. Second, I thank my faculty advisor Dr. Scott Thomson for the help and support that he has given me.

REFERENCES

[1] ADINA User Interface Primer, Report ARD 03-6, June 2003, ADINA R&D Inc. 2003, USA

[2] White,F.,1991, Viscous Fluid Flow 2nd Ed.,McGraw-Hill, Inc.,New York,Chap.4.

APPENDIX

Derivation of Thwaites Method[1]

Thwaites correlation method is an approximate integral method (AIMs). AIMs are derived from the governing equations of continuity and momentum. The final equations are partially integrated forms of continuity and momentum.

Continuity: $$\frac{\partial u}{\partial x}+\frac{\partial v}{\partial y}=0 \qquad \text{eq. 4}$$

Momentum: $$\frac{\partial u}{\partial t}+u\frac{\partial u}{\partial x}+v\frac{\partial v}{\partial y}\approx\left(\frac{\partial U}{\partial t}+U\frac{\partial U}{\partial x}\right)+\frac{1}{\rho}\frac{\partial \tau}{\partial y} \qquad \text{eq. 5}$$

The integral momentum relation is obtained by multiplying continuity by (u-U) and subtracting it from momentum, resulting in the following equation:

$$-\frac{1}{\rho}\frac{\partial \tau}{\partial y}=\frac{\partial(U-u)}{\partial t}+\frac{\partial\left(uU-u^2\right)}{\partial x}+(U-u)\frac{\partial U}{\partial x}+\frac{\partial(vU-vu)}{\partial y} \qquad \text{eq. 6}$$

Allowing unsteady flow and porous walls with v_w(positive for injection), we integrate from the wall to infinity with the result:

$$\frac{\tau_w}{\rho}=\frac{\partial}{\partial t}\int_0^\infty(U-u)\,dy+\frac{\partial}{\partial x}\int_0^\infty\left(uU-u^2\right)dy+\frac{\partial U}{\partial x}\int_0^\infty(U-u)\,dy-Uv_w \qquad \text{eq. 7}$$

This form of the equation is commonly known as the von Kármán integral relation. The integrals of U-u and u(U-u) are exactly the displacement and momentum thicknesses. The displacement and momentum thickness are defined as:

Displacement Thickness δ^*: The distance the stream outside the boundary layer would have to be displaced if the boundary layer were replaced by a uniform flow, while maintaining the mass flow rate.

Momentum Thickness θ: The measure of the deficit in momentum created by inside the boundary layer.

After defining these two quantities the equation can be rewritten in the following form:

$$\frac{\tau_w}{\rho U^2}=\frac{C_f}{2}=\frac{1}{U^2}\frac{\partial\left(U\delta^*\right)}{\partial t}+\frac{\partial\theta}{\partial x}+\left(2\theta+\delta^*\right)\frac{1}{U}\frac{\partial U}{\partial x}-\frac{v_w}{U} \qquad \text{eq. 8}$$

We then make the assumption of steady flow and impermeable wall, and the equation reduces to the most widely used version of the von Kármán equation:

$$\frac{C_f}{2}=\frac{d\theta}{dx}+(2+H)\frac{\theta}{U}\frac{dU}{dx} \qquad H=\frac{\delta^*}{\theta} \qquad \text{eq. 9}$$

Thwaites Correlation Method (White 1994) rewrites the Kármán eq. in terms of a variable called lambda (λ):

$$\lambda=\frac{\theta^2}{\nu}U' \qquad \text{eq. 10}$$

Where θ^2 is the momentum deficit thickness squared and U' is the derivative of the velocity with respect to x. To calculate the necessary values Thwaites proposed that θ^2 could be approximated within ±3 percent by the following equation:

$$\theta^2=\frac{0.45\nu}{U^6}\int_0^x U^5\,dx \qquad \text{eq. 11}$$

Derivation of the Numerical Methods

In order to obtain a value for lambda (λ), equation 11 is calculated numerically using equations 12 and 13. This results in a value for θ^2. Once θ^2 is determined, equation 10 is evaluated numerically using the value for θ^2 and equation 14.

To approximate the integral of the velocity (equation 12) the trapezoidal rule was implemented using the known heights along the surface of the vocal folds. To determine the velocity an initial volumetric flow rate (Q) was set and then the various values calculated (equation 13). Then the separation pressure and minimum pressure ratio was used to iterate to the correct Q. The differentiation of the velocity (equation 14) was determined using a central difference numerical method.

$$\int_0^x U^5\,dx\cong\frac{Q^5}{2}\sum_{i=1}^{n}\left[\left(\frac{1}{H-2*h_i}\right)^5+\left(\frac{1}{H-2*h_{i-1}}\right)^5\right]\left(x_i-x_{i-1}\right) \qquad \text{eq. 12}$$

$$U_i^6=\left(\frac{Q}{H-2*h_i}\right)^6 \qquad \text{eq. 13}$$

$$U'=\frac{Q\left(\frac{1}{H-2*h_{i+1}}-\frac{1}{H-2*h_{i-1}}\right)}{\left(\left(x_{i+1}-x_i\right)+\left(x_i-x_{i-1}\right)\right)} \qquad \text{eq. 14}$$

